PRAMANA
— journal of
physics

Vol. 68, No. 6
June 2007
pp. 967–982

Exact solution of the classical mechanical quadratic Zeeman effect

SAMBHU N DATTA and ANSHU PANDEY*
Department of Chemistry, Indian Institute of Technology – Bombay, Powai, Mumbai 400 076, India
*Present address: Department of Chemistry, University of Chicago, Chicago, IL 60637, USA
E-mail: sndatta@chem.iitb.ac.in

MS received 5 June 2006; accepted 1 March 2007

Abstract. We address the curious problem of quadratic Zeeman effect at the classical mechanical level. The problem has been very well understood for decades, but an analytical solution of the equations of motion is still to be found. This state of affairs persists because the simultaneous presence of the Coulombic and quadratic terms lowers the dynamical symmetry. Energy and orbital angular momentum are still constants of motion. We find the exact solutions by introducing the concept of an image ellipse. The quadratic effect leads to a dilation of space–time, and a one-to-one correspondence is observed for pairs of physical quantities like energy and angular momentum, and the maximum and minimum distances from the Coulomb center for the Zeeman orbit and the corresponding pairs for the image ellipse. Thus, instead of finding additional conserved quantities, we find constants of motion for an additional dynamics, namely, the image problem. The trajectory is open, in agreement with Bertrand's theorem, but necessarily bound. A stable unbound trajectory does not exist for real values of energy and angular momentum. The radial distance, the angle covered in the plane of the orbit, and the time are uniquely determined by introducing further the concept of an image circle. While the radial distance is defined in a closed form as a transcendental function of the image-circular angle, the corresponding orbit angle and time variables are found in the form of two convergent series expansions. The latter two variables are especially contracted, thereby leading to a precession of the open cycles around the Coulomb center. It is expected that the space–time dilation effect observed here would somehow influence the solution of the quantum mechanical problem at the non-relativistic level.

Keyword. Zeeman effect.

PACS No. 32.60.+i

1. Introduction

The quadratic Zeeman effect observed for the hydrogen atom has evoked much interest during the last few decades. Despite a large number of advances made during this period, a complete understanding of even the classical problem is still lacking. The reason for the great difficulty encountered in analytically solving the

quantum mechanical Zeeman problem may be attributed to the fact that a hydrogen atom in a magnetic field exhibits lesser symmetry than a field-free hydrogen atom. A free hydrogen atom can be treated as a four-dimensional harmonic oscillator, which allows the hydrogenic Hamiltonian to be transformed through a variety of techniques [1]. This remains valid when the Zeeman paramagnetic term is included in the Hamiltonian. However, the Zeeman diamagnetic term is inseparable in four dimensions, and this has hindered the development of any exact analytical solution for both the classical and quantum mechanical Zeeman problems. The usual approach adopted in the involved classical treatments relies on the classical perturbation theory.

The quantum mechanical Zeeman problem is likely to be solved if one has the knowledge of additional constants of motion. This is equivalent to the reduction of the order of the differential wave equation through a group of transformations. Since only a few constants of motion, namely, total energy (E) and the parallel component of the orbital angular momentum (L_z) are known till now, all attempted solutions of the Zeeman problem are essentially inexact. Any attempt to solve the quantum mechanical problem must first address the classical problem so that the conserved quantities become precisely known. Nevertheless, certain analytical advances were put forward by Avron *et al* [2], numerical solutions of the non-relativistic quantum mechanical Zeeman problem have been extensively investigated by many authors [3–10], and an approximate constant of motion was found [5].

Recently we have found explicit analytical solutions of the wave equation for a free Dirac particle with an anomalous magnetic moment and moving in a homogeneous magnetic field [11]. The problem of a charged particle in the presence of a Coulomb center and moving in a uniform magnetic field, however, remains unsolved even at the non-relativistic level.

The objective of this paper is to present an exact analytical solution of the classical Zeeman effect. The exact solution identifies the necessary missing link in the form of constants of an additional motion. Besides, the method of solution generates a clarified picture of the classical non-relativistic movement of an overall neutral two-particle system in a homogeneous magnetic field. This paper is arranged as follows. A condensed review of the classical mechanical formulation of the problem is given in §2. The equations of motion are given in §3, and known solutions of these equations in special cases are reviewed in §4. Section 5 describes the qualitative aspects of the solution to the quadratic Zeeman problem. A numerical solution is also illustrated here. In §6 we show that energy, angular momentum, and the maximum and minimum values of the radial distance can be quantitatively determined by using the concept of an image ellipse. Two series expansions are obtained in §7, one for the time variable and the other for the angle in the plane of the orbit, by using the concept of an image circle. The periodic angle can be easily related to the frequency of precession. A short discussion is given in §8.

2. Formulation of the classical problem

Although the classical Hamiltonian function is very well-known, we shall repeat the derivation here for ready reference. This also serves our purpose, for proper

reduced masses have to be used in the treatment. Our starting point is the two-particle classical Hamiltonian function

$$\mathbf{H} = \frac{\pi_1^2}{2m_1} + \frac{\pi_2^2}{2m_2} + V(|\vec{r}_2 - \vec{r}_1|), \tag{1}$$

where $\vec{\pi}_i = \vec{p}_i - q_i\vec{A}_i$ (for $i = 1, 2$). The system is electrically neutral, that is, $q_1 = -q_2 = e_0$. We employ the unit $c = 1$, and use the symmetric gauge $\vec{A}_i = \frac{1}{2}\vec{B} \times \vec{r}_i$ with the magnetic field along the z-axis. Hamilton's equations then yield $\vec{\pi}_i = m_i\dot{\vec{r}}_i$ and $\dot{\vec{p}}_i = -(q_i/2m_i)\vec{B} \times \vec{\pi}_i - \vec{\nabla}_i V$.

The next step involves the separation of the center-of-mass motion. One can define a pseudo-momentum by $\vec{k}_i = \vec{p}_i + q_i\vec{A}_i$, and easily prove $\dot{\vec{k}}_i = -\vec{\nabla}_i V$ so that the total pseudo-momentum $\vec{K} = \vec{k}_1 + \vec{k}_2$ is classically conserved. The center-of-mass and relative coordinates are written as $\vec{R}_{\rm cm} = (m_1\vec{r}_1 + m_2\vec{r}_2)/M$, where $M = m_1 + m_2$ and $\vec{r} = \vec{r}_2 - \vec{r}_1$, respectively. The corresponding linear momentum are $\vec{P}_{\rm cm} = \vec{p}_1 + \vec{p}_2$ and $\vec{p} = (m_1\vec{p}_2 - m_2\vec{p}_1)/M$. A few steps of simplifications along with the choice $\vec{R}_{\rm cm} = \vec{0}$ lead to the reduced Hamiltonian function at zero total pseudo-momentum

$$\mathbf{H}_{\rm red} = \frac{1}{2m_1}(-\vec{p} + e_0\vec{A})^2 + \frac{1}{2m_2}(\vec{p} + e_0\vec{A})^2 + V(r) \tag{2}$$

that describes the movement in relative coordinates. The reduced function can also be written as

$$\mathbf{H}_{\rm red} = \frac{p^2}{2\mu} + \omega_{\rm L}L_z + \frac{\mu}{2}(\omega_{\rm L}^2 + \omega_{\rm L}'^2)(x^2 + y^2) + V(r), \tag{3}$$

where $\omega_{\rm L}$ ($=e_0B/2\mu'$) is the Larmor frequency that needs to be defined in terms of μ', L_z is the z-component of the orbital angular momentum ($\vec{L} = \vec{r}\times\vec{p}$), μ and μ' are two different reduced masses defined as $\mu = m_1m_2/M$ and $\mu' = m_1m_2/(m_1 - m_2)$, and $\omega_{\rm L}' = (\mu'^2/\mu^2 - 1)^{1/2}\omega_{\rm L}$. If one notes $\mu\dot{\vec{r}} = \vec{p} - q\vec{A} = \vec{\pi}$, where $q = -(\mu/\mu')e_0$, one can write

$$\mathbf{H}_{\rm red} = \frac{\pi^2}{2\mu} + \frac{\mu\omega_{\rm L}'^2}{2}(x^2 + y^2) + V(r). \tag{4}$$

We now take into account the angular motion. To do so, we use $\dot{\vec{p}} = -\vec{\nabla}\mathbf{H}_{\rm red}$ and define $\vec{\omega}_{\rm L} = \hat{k}\omega_{\rm L}$ and $\vec{z} = \hat{k}z$ where $\hat{k}$ is the unit vector along the z-axis, and find

$$\begin{aligned}\dot{\vec{L}} &= \vec{\omega}_{\rm L} \times \vec{L} + \mu\Omega_{\rm L}^2\vec{r} \times \vec{z},\\ \Omega_{\rm L} &= (\omega_{\rm L}^2 + \omega_{\rm L}'^2)^{1/2} = e_0B/2\mu.\end{aligned} \tag{5}$$

Therefore, L_z is conserved in time. The occurrence of L_z in (3) indicates that the relative movement can be simplified in a rotating frame of reference. The Lagrangian is found as

$$\begin{aligned}\mathbf{L} &= \vec{p}\cdot\dot{\vec{r}} - \mathbf{H}_{\rm red} \\ &= \mu\dot{r}^2 + \mu\omega_{\rm L}(\dot{x}y - x\dot{y}) - \frac{\mu\omega_{\rm L}'^2}{2}(x^2+y^2) - V(r). \end{aligned} \tag{6}$$

One may introduce the rotating coordinate system ($x' = x\cos\omega_{\rm L}t + y\sin\omega_{\rm L}t, y' = -x\sin\omega_{\rm L}t + y\cos\omega_{\rm L}t, z' = z$ such that $r' = r$) to rewrite the Lagrangian as

$$\mathbf{L}' = \frac{\mu}{2}\dot{r}'^2 - \frac{\lambda}{2}(x'^2 + y'^2) - V(r'), \tag{7}$$

where $\lambda = \mu\Omega_{\rm L}^2$. Now, $\vec{p}' = \mu\dot{\vec{r}}'$ so that the Hamiltonian function in the new coordinate system appears as

$$\mathbf{H}' = \frac{p'^2}{2\mu} + \frac{\lambda}{2}(x'^2 + y'^2) + V(r'). \tag{8}$$

One also observes $\vec{L}' = \vec{r}'\times\vec{p}'$ with $L_x' = L_x\cos\omega_{\rm L}t + L_y\sin\omega_{\rm L}t$, $L_y' = -L_x\sin\omega_{\rm L}t + L_y\cos\omega_{\rm L}t$, and $L_z' = L_z$ such that $L' = L$ and L_z' is a constant of motion.

The dimensionality of the Hamiltonian function $\mathbf{H}'$ is still equal to three, and it can be reduced by using the spherical polar coordinates (r', θ', φ') in the rotating frame. One obtains

$$\begin{aligned}\mathbf{L}' &= \frac{\mu}{2}(\dot{r}'^2 + r'^2\dot{\theta}'^2 + r'^2\sin^2\theta'\dot{\varphi}'^2) - \frac{\lambda}{2}r'^2\sin^2\theta' - V(r'), \\ \mathbf{H}' &= \frac{1}{2\mu}\left(p_{r'}^2 + \frac{p_{\theta'}^2}{r'^2} + \frac{p_{\varphi'}^2}{r'^2\sin^2\theta'}\right) + \frac{\lambda}{2}r'^2\sin^2\theta' + V(r'). \end{aligned} \tag{9}$$

In the above, $p_{r'} = \mu\dot{r}'$, $p_{\theta'} = \mu r'^2\dot{\theta}'$, and $p_{\varphi'} = \mu r'^2\sin^2\theta'\dot{\varphi}' \equiv L_z'$. Since the centrifugal force is in the radial direction, and the Coriolis force is in the $(\vec{r}', \dot{\vec{r}}')$ plane, the motion remains confined to the same plane. Thus, without loss of generality, one can make the choice $\theta' = \pi/2$ such that $\dot{\theta}' = 0$, $p_{\theta'} = 0$, and $\dot{p}_{\theta'} = 0$. This yields a two-dimensional motion that is represented by the functions

$$\begin{aligned}\mathbf{L}' &= \frac{\mu}{2}(\dot{r}'^2 + r'^2\dot{\varphi}'^2) - \frac{\lambda}{2}r'^2 - V(r'), \\ \mathbf{H}' &= \frac{1}{2\mu}\left(p_{r'}^2 + \frac{L_z'^2}{r'^2}\right) + \frac{\lambda}{2}r'^2 + V(r'), \end{aligned} \tag{10}$$

where

$$L_z' = p_{\varphi'} = \mu r'^2\dot{\varphi}'. \tag{11}$$

3. Equation of motion

Hamilton's equations show $\dot{p}_{r'} = L_z'^2/\mu r'^3 - \lambda r' - {\rm d}V/{\rm d}r'$ and $\dot{p}_{\varphi'} = 0$. One can easily obtain the equation of motion

$$\dot{r}' = \left[\frac{2}{\mu}\left(E' - \frac{L_z'^2}{2\mu r'^2} - V - \frac{1}{2}\lambda r'^2\right)\right]^{1/2}. \tag{12}$$

The total energy E' appears as the constant of integration. Combining (11) with (12), one obtains the working equation

$$\frac{\mathrm{d}r'}{\mathrm{d}\varphi'} = r'^2\left[\frac{2\mu}{L_z'^2}\left(E' - \frac{L_z'^2}{2\mu r'^2} - V - \frac{1}{2}\lambda r'^2\right)\right]^{1/2}. \tag{13}$$

For the Zeeman problem, one needs to solve eq. (13) with $V(r') = -\kappa/r'$ where $\kappa = e_0^2$.

4. Special cases

We seek bound state solutions of (13), and exact solutions are known in special cases as reviewed below.

Circular orbits. Circular orbits are always possible. These are obtained by treating r' as independent of φ', and imposing the condition $\mathrm{d}E'/\mathrm{d}r' = 0$ for stability. The results are

$$\begin{aligned} E' &= -\frac{\kappa}{2r'} + \lambda r'^2, \\ L_z' &= [\mu(\kappa r' + \lambda r'^4)]^{1/2}. \end{aligned} \tag{14}$$

Bertrand's theorem specifies that stable (that is, E' is conserved) and closed non-circular orbits are possible only when $\kappa > 0, \lambda = 0$ (the Kepler limit with zero magnetic field) or $\kappa = 0, \lambda > 0$ (the Hooke limit with no r^{-1} potential).

Kepler case ($\lambda = 0$). In this case, eq. (13) can be readily integrated to obtain a stable elliptical orbit (written with double primed quantities) for $e'' < 1$ and $E'' < 0$:

$$\frac{1}{r''} = \frac{1}{a''(1 - e''^2)}(1 + e''\cos\varphi''). \tag{15}$$

The orbit is necessarily closed. The quantities $E'' = -\kappa/2a''$ (<0 and $L_z'' = [\mu\kappa a''(1 - e''^2)]^{1/2}$ completely describe the movement. For $E'' > 0$, one obtains two stable but unbound hyperbolic trajectories with $e'' > 1$,

$$\frac{1}{r''} = \pm\frac{1}{a''(e''^2 - 1)}(1 \mp e''\cos\varphi''), \tag{16}$$

where the plus and minus signs are valid for the ranges $\cos^{-1}(1/e'') \le \varphi'' \le 2\pi - \cos^{-1}(1/e'')$ and $\cos^{-1}(-1/e'') \le \varphi'' \le 2\pi - \cos^{-1}(-1/e'')$ respectively. The corresponding energy and angular momentum are $E'' = \kappa/2a''$ and $L_z'' = [\mu\kappa a''(e''^2 - 1)]^{1/2}$.

Hooke case ($\kappa = 0$). In this case, the integration is again straight-forward and it results in the elliptical path

$$\frac{1}{r''^2} = \frac{1}{a''^2(1-e''^2)}[1 - e''^2\cos^2(\varphi'' - \pi/2)]. \tag{17}$$

In this case, $E'' = (2 - e''^2)\lambda a''^2/2$ (>0 for $\lambda > 0$) and $L''_z = [\mu\lambda(1 - e''^2)]^{1/2}a''^2$. Stable unbound solutions are not possible here with real L''_z. The harmonic force restricts r'' to remain finite for a finite energy.

The reversal of the sign of total energy complicates the issue when both κ and λ are non-zero and positive quantities.

5. The bound state Zeeman problem

We now proceed to solve the general case with $\kappa > 0$ and $\lambda > 0$ that corresponds to the classical Zeeman effect. Note that $\mathrm{d}r'/\mathrm{d}\varphi' = 0$ when either $r' = 0$ (trivial solution) or

$$\lambda r'^4 - 2E'r'^2 - 2\kappa r' + L'^2_z/\mu = 0. \tag{18}$$

Equation (18) has four roots such that (a) all four are real, two are positive and two are negative, (b) only two are real, both positive or both negative, and the other two are complex conjugates or (c) they are two pairs of complex conjugates. For a bound orbit (that is not necessarily closed), there should be at least two real positive roots, say, r'_1 and r'_2. For the same value of r', the absolute magnitude of $\mathrm{d}r'/\mathrm{d}\varphi'$ is the same. Therefore, there is one minimum ($r = r'_1$) and one maximum ($r' = r'_2$), and $r' = f(\varphi')$ is symmetric around both the minimum and the maximum. We get

$$E' = -\frac{\kappa}{r'_1 + r'_2} + \frac{\lambda}{2}(r'^2_1 + r'^2_2),$$
$$L'_z = \left[2\mu\left(\frac{\kappa r'_1 r'_2}{r'_1 + r'_2} + \frac{\lambda}{2}r'^2_1 r'^2_2\right)\right]^{1/2}. \tag{19}$$

For $\lambda \neq 0$, the other two roots of eq. (18) are given by

$$r'_{3,4} = \frac{1}{2}\left[-(r'_1 + r'_2) \pm \left\{(r'_2 - r'_1)^2 - \frac{8\kappa}{\lambda(r'_1 + r'_2)}\right\}^{1/2}\right]. \tag{20}$$

These are indeed either real negative or complex conjugates with a negative real part, and represent spurious solutions. The orbit $r' = f(\varphi')$ is bound as r' varies in the range $r'_1 \leq r' \leq r'_2$. Yet, by Bertrand's theorem, it is open when both κ and λ are positive quantities. A fourth-order Runge–Kutta solution of the equations of motion (12) and (13) is shown in figure 1. This discussion settles the qualitative nature of the trajectory.

6. Solution in terms of the image ellipse

We are interested in finding out an analytical solution of the problem above, with a special view to identify any possible constant of motion besides E' and L'_z. To achieve this end, we make the substitution

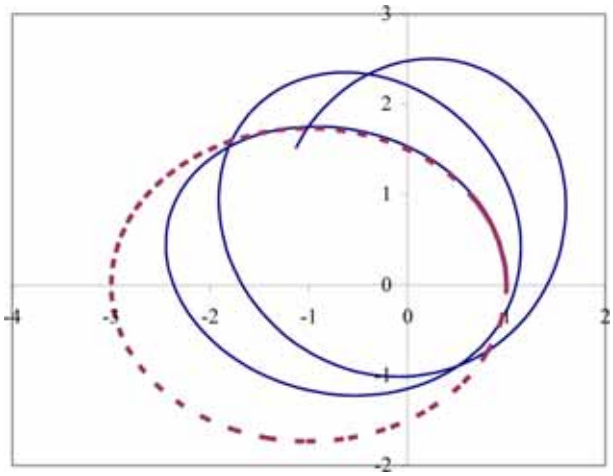

Figure 1. Numerical solution of the trajectory from eqs (12) and (13) for $\kappa = 1$, $\mu = 2$ and $\Omega_{\rm L} = 0.1$. The initial point is $(r' = 1.0083555, \varphi' = 0.0)$ for $t' = 0.0$, and the final point $(r' = 1.8926403, \varphi' = 14.775701)$ is obtained at $t' = 48.0$. The dashed line shows the image ellipse for $a'' = 2$ and $e'' = 0.5$.

$$\left(\frac{\partial\varphi'}{\partial t'}\right)^2_{r'} - \left(\frac{\partial\varphi''}{\partial t''}\right)^2_{r''} = \Omega_{\rm L}^2, \tag{21}$$

where r' and r'' are the corresponding displacements. This gives, in terms of the coordinates (r'', φ'') and time t'', the following quantities:

$$\begin{aligned}
\mathbf{L}'' &= \frac{\mu}{2}(\dot{r}''^2 + r''^2\dot{\varphi}''^2) + \frac{\kappa}{r''}, \\
\mathbf{H}'' &= \frac{1}{2\mu}\left(p_{r''}^2 + \frac{L_z''^2}{r''^2}\right) - \frac{\kappa}{r''}, \\
p_{\varphi''} &= \mu r''^2\dot{\varphi}'' \equiv L_z''.
\end{aligned} \tag{22}$$

The solution is an image ellipse of the form of (15). The corresponding E'' and L_z'' have been quoted right after the same equation. The minimum $\dot{\varphi}'$ (for $r' = r_2'$) corresponds to the minimum $\dot{\varphi}''$ (for $r'' = r_2'' = a''(1 + e'')$), and the maximum $\dot{\varphi}'$ (for $r' = r_1'$) corresponds to the maximum $\dot{\varphi}''$ (for $r'' = r_1'' = a''(1 - e'')$). But the distances r' and r'' are different as time variables t' and t'' are, that is, the maxima and minima for the open trajectory and the image ellipse occur at different distances and different instants of time. The image ellipse for the parameters chosen for figure 1 is shown by the dashed line in the same figure.

From eq. (21) and the definitions of L_z' and L_z'', we get the relationship between the corresponding displacements,

$$r'^4 = \frac{L_z'^2 r''^4}{L_z''^2 + \mu\lambda r''^4}. \tag{23}$$

Also,

Table 1. Characteristics of the bound state solutions of the Zeeman problem for different magnetic field strengths. All solutions correspond to the same image ellipse with $a'' = 2$ and $e'' = 0.25$. We have taken $\kappa = 1$ and $\mu = 2$.

$\Omega_{\rm L}$	ρ	r'_1	r'_2	L'_z	E'
0.00	1.66667	1.50000	2.50000	1.93649	−0.50000
0.01	1.66516	1.50031	2.49825	1.93781	−0.24924
0.10	1.54790	1.52521	2.36087	2.05549	−0.17833
1.00	1.03722	1.66979	1.73195	6.07084	5.49388
10.0	1.00040	1.68441	1.68509	56.7971	567.378
∞[a]	1.00000	1.68457	1.68457	∞	∞

[a]Limit behavior.

$$r'_2 = \rho r'_1 \tag{24}$$

where the ratio ρ is given by

$$\rho = \left(\frac{L''^2_z / a''^4 (1-e'')^4 + \mu\lambda}{L''^2_z / a''^4 (1+e'')^4 + \mu\lambda} \right)^{1/4}. \tag{25}$$

Besides,

$$\begin{aligned} E' &= \frac{L'^2_z}{2\mu r'^2_1} + \frac{1}{2}\lambda r'^2_1 - \frac{\kappa}{r'_1}, \\ L'^2_z &= \frac{2\mu\rho^2}{1+\rho}\left(\frac{1}{2}\lambda(1+\rho) r'^4_1 + \frac{\kappa}{\rho} r'_1 \right). \end{aligned} \tag{26}$$

These relations lead to the result

$$r'_1 = \left(\frac{2\mu\kappa\rho}{(1+\rho)[L''^2_z / a''^4 (1-e'')^4 + (1-\rho^2)\mu\lambda]} \right)^{1/3}. \tag{27}$$

Equations (23)–(27) give complete solutions for ρ and r'_1, and hence r', E' and L'_z in terms of the parameters a'' and e'' of the image ellipse.

For a given κ and μ, a unique set of parameters (a'', e'') defines a unique set of values (E'', L''_z) and an initial condition (such as $r'' = a''(1-e'')$ and $\varphi'' = 0$ at $t'' = 0$) leads to a unique elliptical path. If one also specifies a non-zero $\Omega_{\rm L}$, one obtains a unique set of values (E', L'_z). A given starting point (such as $r' = r'_1$ and $\varphi' = 0$ at $t' = 0$) leads to a unique trajectory $[r'(t'), \varphi'(t')]$. Table 1 contains a few prototype results for different magnetic field strengths.

The ratio ρ can again be expressed as

$$\rho = \left[\left(\frac{1+e''}{1-e''} \right)^3 \frac{(1+e'')\kappa + (1-e'')^3 \lambda a''^3}{(1-e'')\kappa + (1+e'')^3 \lambda a''^3} \right]^{1/4}. \tag{28}$$

The limiting values are

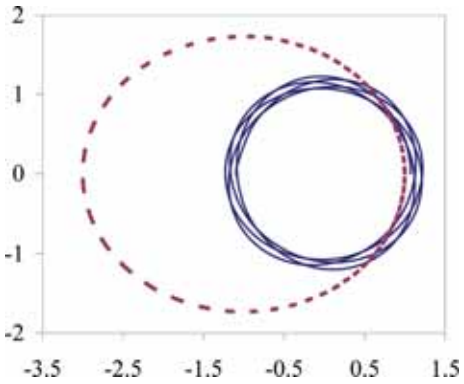

Figure 2. The quadratic Zeeman trajectory for $\kappa = 1, \mu = 2$ and $\Omega_{\rm L} = 1.0$. The initial point is $(r' = 1.0724469, \varphi' = 0.0)$ for $t' = 0.0$, and the final point $(r' = 1.0935972, \varphi' = 28.2920595)$ is obtained at $t' = 24.5$. The dashed line shows the image ellipse for $a'' = 2$ and $e'' = 0.5$.

$$\rho = \frac{1+e''}{1-e''} - 2\frac{\lambda a''^3}{\kappa}\frac{e''(1+e''^2)}{(1-e'')^2} \tag{29a}$$

as $\lambda a''^3/\kappa \to 0$, and

$$\rho = 1 + 2\frac{\kappa}{\lambda a''^3}\frac{e''(1+e''^2)}{(1-e''^2)^3} \tag{29b}$$

as $\kappa/\lambda a''^3 \to 0$. Thus ρ decreases from $(1+e'')/(1-e'')$ to 1 as the magnetic field strength increases from 0 to ∞. The orbit becomes increasingly circular. This can be clearly seen by comparing figure 1 with figure 2.

7. Image circle, angle and time

The variables φ' and t' are obtained from a consideration of the image circle.

To know the time dependence of r'' and φ'' for the Kepler ellipse, one introduces a new variable η'' such that

$$r'' = a''(1 - e''\cos\eta''). \tag{30}$$

A specification of η'' as a function of t'' completely specifies r'' and hence φ''. We find

$$t'' = \left(\frac{\mu a''^3}{\kappa}\right)^{1/2}(\eta'' - a''e''\sin\eta''), \tag{31}$$

$$\varphi'' = \cos^{-1}\left(\frac{\cos\eta'' - e''}{1 - e''\cos\eta''}\right), \tag{32}$$

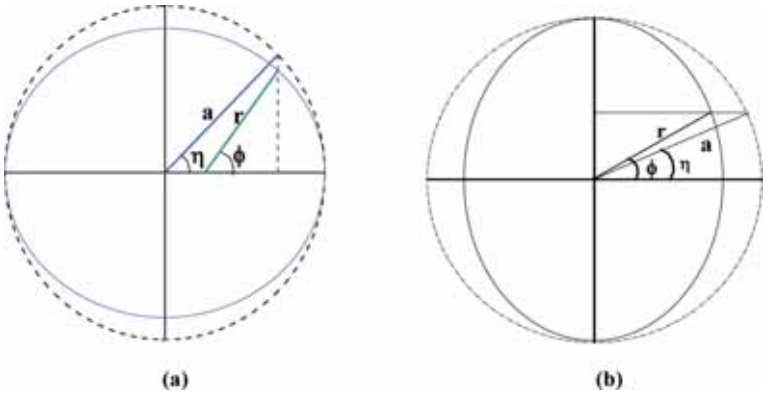

Figure 3. The image circle (dashed line) for (**a**) the Kepler ellipse and (**b**) the Hooke ellipse.

and the time period for the repeat of the minimum r'' (or the maximum distance) as

$$T'' = 2\pi(\mu a''^3/\kappa)^{1/2}. \tag{33}$$

The angle η'' is the angle on the image circle of the image ellipse as shown in figure 3a with $a'' = 2$ and $e'' = 0.25$. Figure 3a completely defines r'', φ'' and t''. The image circle for the Hooke solution is shown in figure 3b. A numerical solution of η'' as a function of t'' can be obtained from (31), and the solution is illustrated in figure 4.

The image circle for the Hooke solution is more familiar. One writes

$$r'' = a''[1 - e''^2 \cos^2 \eta'']^{1/2} \tag{34}$$

to get

$$\eta'' = \left(\frac{\lambda}{\mu}\right)^{1/2} t'', \tag{35}$$

$$\varphi'' = \sin^{-1}\left(\frac{\sin\eta''}{\sqrt{1 - e''^2\cos^2\eta''}}\right),$$

$$T'' = \pi(\mu/\lambda)^{1/2}.$$

where $a'' = 2$ and $e'' = 0.25$.

One can similarly create an image circle description for the Zeeman bound state trajectory given by (12) by writing

$$r' = a'(1 - e'\cos\eta'), \tag{36}$$

where $a' = (1+\rho)r'_1/2$ and $e' = (\rho - 1)/(\rho + 1)$, and find after some calculation

$$\frac{a'(1 - e'\cos\eta')\mathrm{d}\eta'}{\left[\frac{\kappa}{a'} + \lambda a'^2\{(2 - e'\cos\eta')^2 - e'^2\}\right]^{1/2}} = \frac{1}{\mu^{1/2}}\mathrm{d}t'. \tag{37}$$

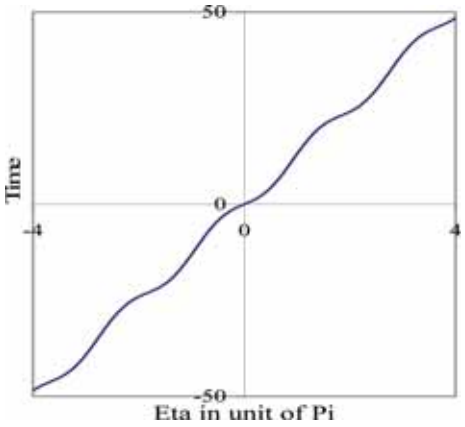

Figure 4. Variation of time t'' with the image circle angle η'' for a Kepler ellipse with $a'' = 2$ and $e'' = 0.25$. We have also taken $\kappa = 1$ and $\mu = 2$. For the Hooke ellipse, the image circle angle varies linearly with time.

A solution of t' as a function of η' can be obtained by expanding the left side in terms of increasing powers of ζ where

$$\zeta = \frac{\lambda a'^2}{\xi} \tag{38}$$

and

$$\xi = \frac{\kappa}{a'} + \left(4 - \frac{e'^2}{2}\right)\lambda a'^2. \tag{39}$$

One finds

$$t' = a'\left(\frac{\mu}{\xi}\right)^{1/2}\left[\eta' - e'\sin\eta' + \sum_{n=1}^{\infty}\frac{(2n-1)!!(2e'\zeta)^n}{n!} \times \sum_{m=0}^{n}\frac{(-1)^m}{2^{2m}}\binom{n}{m}\{e'^m\mathcal{I}_{m+n}(\eta') - e'^{m+1}\mathcal{I}_{m+n+1}(\eta')\}\right], \tag{40}$$

where

$$\mathcal{I}_p(\eta') = \int_0^{\eta'} \mathrm{d}\eta\cos^p\eta = \frac{1}{2^{p-1}} \times \sum_{q=0}^{(p-1)/2}\binom{p}{q}\frac{\sin(p-2q)\eta'}{(p-2q)} \quad (\text{for } p = \text{odd}),$$

$$\mathcal{I}_p(\eta') = \frac{1}{2^{p-1}}\sum_{q=0}^{p/2-1}\binom{p}{q}\frac{\sin(p-2q)\eta'}{(p-2q)} + \frac{1}{2^p}\binom{p}{p/2}\eta' \quad (\text{for } p = \text{even}). \tag{41}$$

As λ varies from 0 to infinity, ζ varies from 0 to 1/4 and e' varies from e'' to 0. The product $e'\zeta$ is always less than $e''/4$. Therefore, (40) converges rapidly and for each η', a unique set of (r', t') is obtained. The time period (T') occurs at $\eta' = 2\pi$:

$$T' = 2\pi a' \left(\frac{\mu}{\xi}\right)^{1/2} \left[1 + \sum_{n=1}^{\infty} \frac{(2n-1)!!(e'\zeta)^n}{n!} \sum_{m=0}^{n} \frac{(-e')^m}{2^{3m}} \begin{pmatrix} n \\ m \end{pmatrix} \times \left\{ \begin{pmatrix} m+n \\ (m+n)/2 \end{pmatrix} \delta_{m+n,2[(m+n)/2]} - \frac{e'}{2} \begin{pmatrix} m+n+1 \\ (m+n+1)/2 \end{pmatrix} \delta_{m+n+1,2[(m+n+1)/2]} \right\} \right]. \quad (42)$$

It is easy to verify that the Kepler and Hooke time periods are indeed retrieved in the limits $\lambda a'^3/\kappa \to 0$ and $\kappa/\lambda a'^3 \to 0$ (with $e' \to 0$), respectively.

The fifth order term in (42) has a factor $\zeta^5 e'^6$. For $e'' = 0.25, e' < 0.25$ and a fourth-order expansion is sufficient to ensure a six-digit accuracy. Calculated time periods for $\mu = 2, \kappa = 1, a'' = 2$ and $e'' = 0.25$ are given in table 2 for various $\Omega_{\rm L}$.

This still leaves φ' to be calculated. This is accomplished by combining (36) and (37) with the definition of L'_z. We get

$$\varphi' = \frac{L'_z}{a'(\mu\xi)^{1/2}} \left[\mathcal{F}(\eta') + 2\pi \sum_{n=1}^{\infty} \frac{(2n-1)!!(2e'\zeta)^n}{n!} \times \sum_{m=0}^{n} \left(-\frac{e'}{4}\right)^m \begin{pmatrix} n \\ m \end{pmatrix} \Im_{m+n}(\eta') \right], \quad (43)$$

where the integrals $\mathcal{F}$ and $\Im$ are given by

$$\mathcal{F}(\eta') = \int_0^{\eta'} \frac{\mathrm{d}\eta}{1 - e'\cos\eta} = \eta' + \sum_{q=1}^{\infty} e'^q \mathcal{I}_q(\eta') \quad (44)$$

and

$$\Im_p(\eta') = \frac{1}{2\pi} \int_0^{\eta'} \frac{\cos^p \eta}{1 - e'\cos\eta} \mathrm{d}\eta = \frac{1}{2\pi} \sum_{q=0}^{\infty} e'^q \mathcal{I}_{p+q}(\eta'). \quad (45)$$

Special values are

$$\mathcal{F}(2\pi) = \frac{2\pi}{\sqrt{1-e'^2}} \quad (46)$$

and

$$\Im_0(2\pi) = 1$$
$$\Im_{2p-1}(2\pi) = \frac{e}{2^{2p}} \begin{pmatrix} 2p \\ p \end{pmatrix} \times \left\{1 + \left(\frac{e^2}{2}\right) \frac{(2p+1)}{(p+1)} + \left(\frac{e^2}{2}\right)^2 \frac{(2p+1)(2p+3)}{(p+1)(p+2)} + \cdots \right\},$$
$$\Im_{2p}(2\pi) = \Im_{2p-1}/e. \quad (47)$$

An important quantity is the periodic angle φ'_c that is covered between two successive minimum distances ($\varphi = \varphi'_c$ when $\eta' = 2\pi$). For the Kepler ellipse, $\varphi''_c = 2\pi$ while for the Hooke orbit, $\varphi''_c = \pi$. For quadratic Zeeman effect, φ'_c varies from 2π to π as $\Omega_{\rm L}$ increases. We find

$$\varphi'_c = \frac{2\pi L'_z}{a'(\mu\xi)^{1/2}} \left[\frac{1}{\sqrt{1-e'^2}} + \sum_{n=1}^{\infty} \frac{(2n-1)!!(2e'\zeta)^n}{n!} \times \sum_{m=0}^{n} \left(-\frac{e'}{4}\right)^m \begin{pmatrix} n \\ m \end{pmatrix} \Im_{m+n}(2\pi) \right]. \tag{48}$$

Again, for $e'' = 1/4$, a six-digit accuracy is obtained from the fourth-order expansion (table 2).

That φ'_c is found between π and 2π leads to a precession of cycles. The precession frequency $\omega_{\rm P}$ can be written as $\omega_{\rm P} = (\varphi'_c - 2\pi)/T'$, the negative sign implying that the direction of precession (clockwise) is opposite to the direction of rotation (anticlockwise) around the Coulomb center (as shown in figure 1). A typical precession is selected for illustration in figure 5 where the orbit more or less closes after 9 cycles accompanied by a precession through -2π. The trajectory in figure 5 is based on the same set of parameters used for figure 1 ($\kappa = 1, \mu = 2, \Omega_{\rm L} = 0.1, a'' = 2.0$ and $e'' = 0.5$), but the total time used is in excess of 155.4 unit. The same diagram can be generated from eqs (36) and (43). For the chosen parameters, the values calculated from eqs (42) and (48) are indeed $T' = 17.2657$ and $\varphi'_c = 1.77668\pi$ so that $\omega_{\rm P} = -0.0406346$ per unit time. Since φ'_c is almost equal to $16\pi/9$, the orbit almost closes after 9 cycles and at a time gap of 155.391 unit. After nine cycles of rotation, the orbit angle covered deviates from 16π by less than 0.01π, and the deviation of the trajectory from the original one becomes visible only after several complete cycles of precession. The rate of precession increases with the increase in magnetic field, and at a very high field approaches $\Omega_{\rm L}$ (table 2). This can also be seen by comparing figure 2 (for $\Omega_{\rm L} = 1.0$) with figure 5 (for $\Omega_{\rm L} = 0.1$).

8. Results and discussion

Equation (21) has been the critical step in our derivation, and it leads to a dilation of space–time. The Zeeman trajectory can be obtained from any image ellipse specified by a'' and e''. A unique set (E', L'_z) and another unique set (r'_1, r'_2) are obtained for a specific $\Omega_{\rm L}$. The values r'_1 and r'_2 give a' and e', and a unique r' can be obtained as a function of the circular angle η'. The time t' and the angle φ' can be calculated by numerically integrating eqs (12) and (13) respectively. Alternatively, time and angle can be determined from the power series expansions (40) and (43) respectively.

Tables 1 and 2 are based on the image ellipse of eccentricity 0.25, whereas for figures 1, 2 and 5, the image eccentricity used is 0.5. The quadratic Zeeman orbit always lies in the annular belt defined by $r'_1 \le r' \le r'_2$.

For $E' < 0$, the trajectory is more like a distorted Kepler ellipse, but for $E' > 0$ the orbit is mainly Hooke-like. The quadratic term leads to topologically distinct

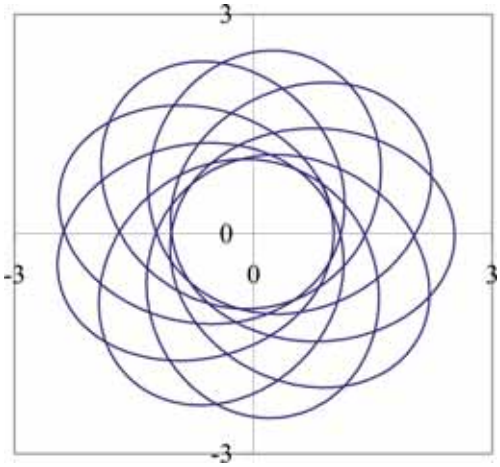

Figure 5. Precession of the quadratic Zeeman orbit in rotating coordinates. The orbit more or less closes after 9 cycles.

kinds of dynamics in a quantum mechanical treatment [5,9]. In the classical situation, the transition from a Kepler-type motion to a Hooke-like one is not sharp. It is approximately characterized by the crossover point $E' = 0$ that occurs when

$$\rho^3 + \rho^2 + \rho - \frac{\kappa}{\lambda a''^3}\frac{(1+e'')}{(1-e'')^3} = 1. \tag{49}$$

In view of eq. (25), the crossover point is given by

$$\frac{[(\rho^3-1)-\rho(\rho+1)]}{\rho^3[(\rho^3-1)+\rho(\rho+1)]} = -\left(\frac{1-e''}{1+e''}\right)^4. \tag{50}$$

For $e'' = 0.25$, the crossover is found at $\rho_0 = 1.37808$. The important ratio is $\kappa/\lambda a''$ at zero energy, that is found to be 1.65183 for $e'' = 0.25$. For $a'' = 2, \kappa = 1$ and $\mu = 2$ as used in table 1, the following quantities are obtained: $\lambda = 0.07567, \Omega_{\rm L} = 0.19452, r_1' = 1.56506, r_2' = 2.15679$, and $L_z' = 2.31349$. For a more realistic situation in atomic physics, we choose the atomic units $e_0 = 1, \mu = 1$ and $\hbar = 1$ such that $c = \alpha^{-1}, \alpha$ being the fine structure constant. For $a'' = x^2 a_0$ where a_0 is the unit of length, we find $\Omega_{\rm L} = 0.778068x^{-3}$ in atomic unit. The normalized magnetic field given by $\gamma = \hbar\Omega_{\rm L}/{\rm Ry}$ where Ry stands for one Rydberg or half of atomic unit of energy turns out to be $1.55614x^{-3}$. For instance, if $x = 2$, then $\gamma = 0.194517$. In the quantum mechanical case, many level crossings occur and the energy values of all states barring the 1s become positive in the region $0 < \gamma < 1$ [3].

The nature of the roots of eq. (18) discussed in §5 precludes the possibility of any stable unbound solution of the quadratic Zeeman problem as the real positive roots always occur in pairs and are finite. This is again the outcome of the presence of the harmonic potential. If one starts from a Kepler hyperbola (with $E'' > 0$ and $\lambda = 0$) and ascribes a small positive value to λ, eq. (12) yields a rapidly decreasing

Table 2. The periodic amplitude, time period and precession frequency in classical quadratic Zeeman effect. All solutions correspond to the same image ellipse with $a'' = 2$ and $e'' = 0.25$. We have taken $\kappa = 1$and $\mu = 2$.

$\Omega_{\rm L}$	φ'_c/π	T'/π	$\omega_{\rm P}$
0.00	2.00000	8.00000	0.000000
0.01	1.99538	7.96967	−0.000580
0.10	1.70629	6.06905	−0.048393
1.00	1.03644	0.987534	−0.975720
10.0	1.00039	0.0999869	−9.99739
∞[a]	1.00000	$\Omega_{\rm L}^{-1}$	$-\Omega_{\rm L}$

[a]Limit behavior.

$\dot{r}'$ as r' increases. The result is that the arms of the hyperbolic trajectory bend towards the major axis and leads to the formation of the open stable trajectory with $E' > 0$.

The main feature of the quadratic Zeeman effect is presented here as the dilated space–time. The angle variable and the time variable are especially contracted. A unique correspondence is observed between (E'', L''_z) and (E', L'_z) for a given $\Omega_{\rm L}$ in the classical Zeeman effect. The implication of this correspondence in the quantum mechanical situation remains to be explored [12]. The best analytical solution of the quantum Zeeman problem was derived by Praddude [3] who observed a one-to-one correspondence between the Zeeman wave functions (characterized by four quantum numbers) at zero magnetic field and the standard hydrogen atom wave functions (characterized by three quantum numbers). Praddude mixed radial functions and expanded the mixed function in an infinite series, and therefore had to solve an infinite set of linear algebraic equations. This eluded the derivation of eigenfunctions and eigenvalues in closed forms.

Acknowledgment

SND is grateful to CSIR for financial support.

References

[1] F H J Cornish, *J. Phys.* **A17**, 323 (1984)
[2] J E Avron, W Herbst and B Simon, *Ann. Phys.* **114**, 431 (1978)
[3] H C Praddaude, *Phys. Rev.* **A6**, 1321 (1972)
[4] M L Zimmerman, M M Kash and D Kleppner, *Phys. Rev. Lett.* **43**, 1092 (1980)
[5] D Herrik, *Phys. Rev.* **A26**, 323 (1982)
[6] M A Al-Laithy, C M Farmer and M R C McDowell, *Phys. Lett.* **A108**, 144 (1985)
[7] G Hose, H S Taylor and D Richards, *J. Phys.* **B18**, 51 (1985)
[8] S Saini and D Farrelly, *Phys. Rev.* **A36**, 3556 (1987)
[9] K D Krantzmann, J A Miligan and D Farrelly, *Phys. Rev.* **A45**, 3093 (1992)
[10] E Oks, *Eur. Phys. J.* **D28**, 171 (2004)

[11] S N Datta and A Misra, *Int. J. Quantum Chem.* **82**, 209 (2001)
[12] A word of caution is added here. Equation (21) is used to obtain the Lagrangian of the image problem, and then the Hamiltonian is worked out. The final result is an increase in energy from the energy of the image orbit. The quantum mechanical counterpart of the image ellipse corresponds to the solution of the Zeeman paramagnetic wave equation in a rotating coordinate system. It would be traditional to use the Ω_{L} containing term as a perturbation in a low magnetic field while the Zeeman paramagnetic Hamiltonian constitutes the zeroth order operator. Again, a general effect is an increase in energy because of the first-order correction